

Article

Free Vibration Analysis of Curved Laminated Composite Beams with Different Shapes, Lamination Schemes, and Boundary Conditions

Bin Qin ^{1,2,3}, Xing Zhao ^{4,*}, Huifang Liu ^{1,2,3}, Yongge Yu ⁵ and Qingshan Wang ⁴

¹ Key Laboratory of Traffic Safety on Track, Ministry of Education, School of Traffic & Transportation Engineering, Central South University, Changsha 410075, China; qinbin@csu.edu.cn (B.Q.); liuhf_csu@163.com (H.L.)

² Joint International Research Laboratory of Key Technology for Rail Traffic Safety, Central South University, Changsha 410075, China

³ National & Local Joint Engineering Research Center of Safety Technology for Rail Vehicle, Central South University, Changsha 410075, China

⁴ State Key Laboratory of High Performance Complex Manufacturing, Central South University, Changsha 410083, China; qingshanwang@csu.edu.cn

⁵ Overall R&D Department, CRRC Changchun Railway Vehicles Co. LTD, Changchun 130062, China; yuyongge.a@cccar.com.cn

* Correspondence: xingzhao@csu.edu.cn

Received: 7 January 2020; Accepted: 18 February 2020; Published: 24 February 2020



Abstract: A general formulation is considered for the free vibration of curved laminated composite beams (CLCBs) with alterable curvatures and diverse boundary restraints. In accordance with higher-order shear deformation theory (HSDT), an improved variational approach is introduced for the numerical modeling. Besides, the multi-segment partitioning strategy is exploited for the derivation of motion equations, where the CLCBs are separated into several segments. Penalty parameters are considered to handle the arbitrary boundary conditions. The admissible functions of each separated beam segment are expanded in terms of Jacobi polynomials. The solutions are achieved through the variational approach. The proposed methodology can deal with arbitrary boundary restraints in a unified way by conveniently changing correlated parameters without interfering with the solution procedure.

Keywords: modified variational approach; curved laminated composite beams; Jacobi polynomials; alterable curvatures; multi-segment partitioning strategy

1. Introduction

The moderately tall curved laminated composite beams (CLCBs) are widely applied in engineering fields. Besides, the laminated composite material has excellent mechanical properties including high compression-resistance capacity, high strength-to-weight and stiffness-to-weight ratios, preeminent corrosion-resistance, and powerful customizable capacity [1,2]. In practical use, the CLCBs may commonly undergo various kinds of complicated dynamic loads and other complex work environments, which lead to excessive vibration and fatigue damage of the structure. Dynamic modelling is the precondition for understanding the vibration characteristics of CLCBs. Thus, this paper aims to evaluate the vibration features of CLCBs with alterable curvatures by a modified variational approach in the framework of higher-order shear deformation theory (HSDT).

Numerous works have been carried out on the vibration problems of CLCBs. A group of equations were constructed by Qatu [3] for vibration analysis of simply supported CLCBs, which

are thin or moderately tall. The influences of rotary inertia, shear deformation, thickness ratio, material orthotropy, and curvature on the vibration frequencies were investigated. Utilizing the Ritz method, Qatu [4,5] implemented dynamic analysis of CLCBs with shallow and deep curvatures. The in-plane vibration characteristics were investigated. By the dynamic stiffness approach in conjunction with series solutions, vibration analysis of curved laminate beams was conducted by Tseng et al. [6]. The impacts of rotary inertia, as well as shear deformation, were taken into account for the numerical model. A novel layer-wise displacement model was put forward by Carpentieri et al. [7] to capture the dynamic behaviors of CLCBs subjected to classic restraints. In the framework of shallow shell theory assumptions, a modal method was proposed by Khdeir and Reddy [8] to unearth the dynamic features of a shallow laminated composite arch subjected to various boundary restraints. Surana and Nguyen [9] proposed a two-dimensional (2D) element formulation for the dynamic analysis of a curved beam by utilizing HSDT. Exploiting first-order shear deformation theory (FSDT), the dynamic behavior of simply supported CLCBs with deep curvatures was studied by Hajianmaleki and Qatu [10]. The general differential quadrature method (DQM) was adopted for the formulation. The vibration features of curved delaminated composite beams were studied by Jafari et al. [11] via a finite element approach and analytical solution. The influences of rotary inertia, material coupling, shear deformation, and the deepness term were taken into consideration. On the foundation of 2D elasticity theory, the vibration features of CLCBs were investigated by Chen et al. [12], where the state space approach and DQM method were employed. A one-dimensional (1D) mechanical model was considered by Ascione and Fraternali [13] for dynamic analysis of CLCBs. The model was constructed based on the stationary potential energy theory, and penalty terms were employed to impose the restraint conditions. Only classic boundary conditions were taken into account. The vibration features of deep CLCBs subjected to various boundary conditions were analyzed by Ye et al. [14] through the Ritz method, where the improved Fourier series was used for the admissible displacement functions. Based on NURBS (Non-Uniform Rational B-Splines), isogeometric analysis was implemented by Luu et al. [15] for understanding the dynamic behaviors of Timoshenko-type deep curved laminated beams with various curvatures. The instantaneous responses of curved composite laminated beams were studied by Shao et al. [16], where the reverberation ray matrix approach was introduced. The curved beams were subjected to arbitrary boundary restraints and diverse lamination schemes were considered. A general and unified formulation was proposed by Qu et al. [17] for vibration analysis of CLCBs subjected to diverse boundary restraints. The modified variational principle was used for the derivation of the formulation, and a multi-segment partitioning strategy was employed. The vibration characteristics of glass fiber-reinforced polymer (GFRP) composites reinforced with nylon nano-fibers were experimentally and numerically studied by Garcia et al. [18,19]. Recently, the spectral-Tchebychev technique, which utilizes Tchebychev polynomials for the spatial discretization, has been proposed by several researchers [20–22]. The method incorporates different boundary conditions by projection matrices, where solutions for various linear and nonlinear vibration problems with different boundary conditions can be easily obtained.

The development of calculating methods of high precision has become an important subject, and multitudinous beam theories and calculation methods have been developed on the foundation of diverse assumptions and approximations. From a literature review, it has been found that most previous investigations about the free vibration of CLCBs have been confined to classical boundary restraints. For accurate beam theories, three major categories are adopted, commonly including classical, first-order, and higher-order beam theories. The classical beam theory (CBT) is suitable for slender beams. As the influence of the transverse shear deformation is ignored by CBT, the deflection is underestimated and the natural frequency is overestimated for tall beams. To make up for this deficiency, the first-order beam theory (FBT) was developed. For FBT, a shear correction factor is introduced to express the transverse shear force, the values of which are affected by a lot of parameters (e.g., layer sequences, material properties, etc.) and which will significantly affect the accuracy of the results. To further improve and perfect the beam theory, the HSDT was developed. Compared to

CBT and FBT, HSDT can express the kinematics of the CLCB better and can produce more precise interlaminar stress distributions. Besides, the shear deformation effects are considered for HSDT, which includes the correct cross-sectional warping without the requirement of a shear correction factor. However, HSDT involves higher-order stress resultants and, thus, needs a higher computational cost, which is one limitation of the present approach.

In addition, the majority of studies have been conducted on the vibration features of circular CLCBs, while those of others are rare. The reason for this is that when the curvature radius is changed, the more complex description of the geometry will make the solution become very difficult [23]. On the whole, investigations of the free vibration of CLCBs subjected to arbitrary boundary restraints and with alternate curvatures are limited. This paper proposes a general and unified formulation for vibration analysis of CLCBs with various curvatures. The novelties of the present paper are as follows: (1) First, most of the previous studies concerned curved circular composite laminated beams (Qu et al. [17]), while studies of CLCBs with various curvatures are rare; (2) a variational method in conjunction with a multi-segment partitioning strategy and HSDT for CLCBs is presented, which has the following advantages: (a) Allowing flexible choices of admissible functions, (b) fast and stable convergence characteristics, and (c) high accuracy, especially for higher modes; (3) the penalty and boundary parameters are incorporated for the convenient change of boundary conditions including classic and elastic ones. On the whole, this approach should be valuable in both theoretical and engineering aspects. The outline of the paper is divided into three parts: (1) Theoretical formulations; (2) results and discussions; and (3) conclusions.

2. Theoretical Formulations

2.1. Description of the CLCB Model

The schematic plot and geometric parameters of a CLCB are presented in Figure 1. The curved beam has curvature radius R_φ , thickness h , and width b . The orthogonal coordinates (φ, y, z) are located at the middle surface of the CLCB. The φ -, y -, and z - coordinates are along the central line (indicated as red line), width, and thickness orientations, respectively. The curved beam comprises several orthotropic layers, where Z_k represents the distance from the top surface of the k 'th layer to the middle surface. The fiber orientation angle of the k 'th lamina with respect to the φ -axis of the CLCBs is defined as α_{fiber}^k , and the case of $\alpha_{fiber}^k = 0$ is presented for a better understanding. Vibration of the CLCB occurs in the φ - z plane and can be characterized by the central line. In engineering applications, different types of CLCBs with diverse curvatures may be encountered, e.g., hyperbolic, parabolic, elliptic, and circular ones. For each type, their radii of curvatures $R_\varphi(\varphi)$ can be described in terms of different geometric parameters. Different types of CLCBs are shown in Figure 2; note that the x -axis, which is perpendicular to the z -axis in the φ - z plane, is added for a better description.

For an elliptic curved beam (Figure 2a), $R_\varphi(\varphi)$ is defined in terms of semimajor axis length a_e and semiminor axis length b_e :

$$R_\varphi(\varphi) = \frac{a_e^2 b_e^2}{\sqrt{(a_e^2 \sin^2 \varphi + b_e^2 \cos^2 \varphi)^3}}. \quad (1)$$

For a parabolic curved beam (Figure 2b), $R_\varphi(\varphi)$ can be expressed as

$$R_\varphi(\varphi) = \frac{k}{2 \cos^3 \varphi}, k = \frac{R_1^2 - R_0^2}{L}, \varphi_0 = \arctan\left(\frac{2R_0}{k}\right), \varphi_1 = \arctan\left(\frac{2R_1}{k}\right), \quad (2)$$

where R_0 and R_1 indicate the horizontal radius.

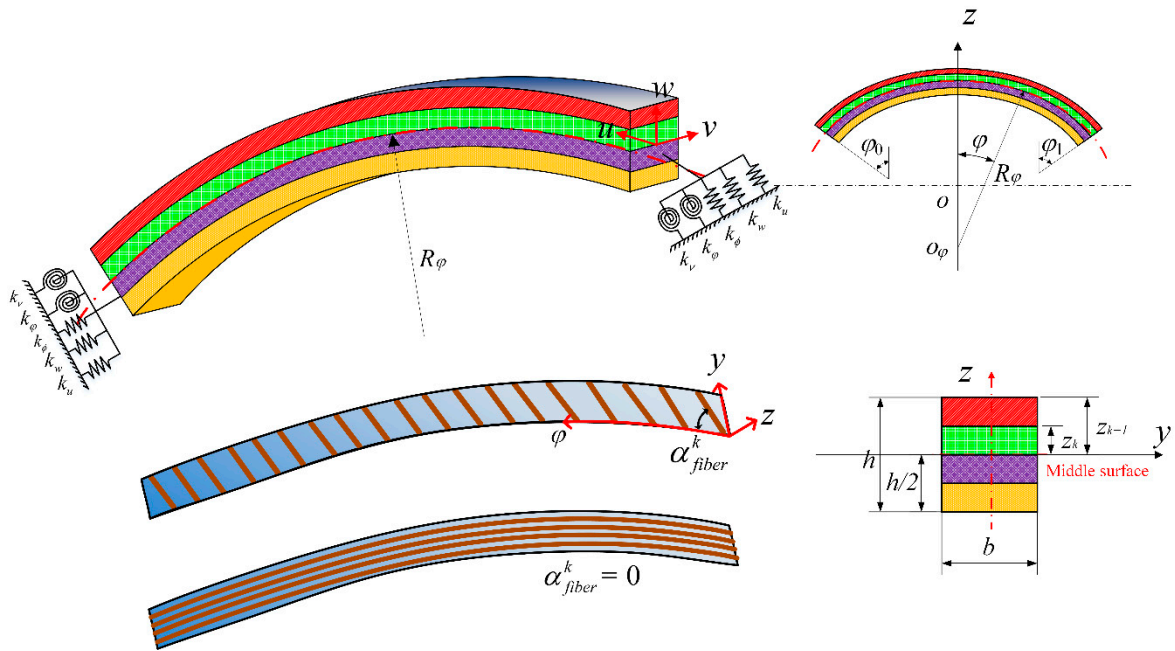


Figure 1. Schematic plot and geometric parameters of curved composite laminated beams.

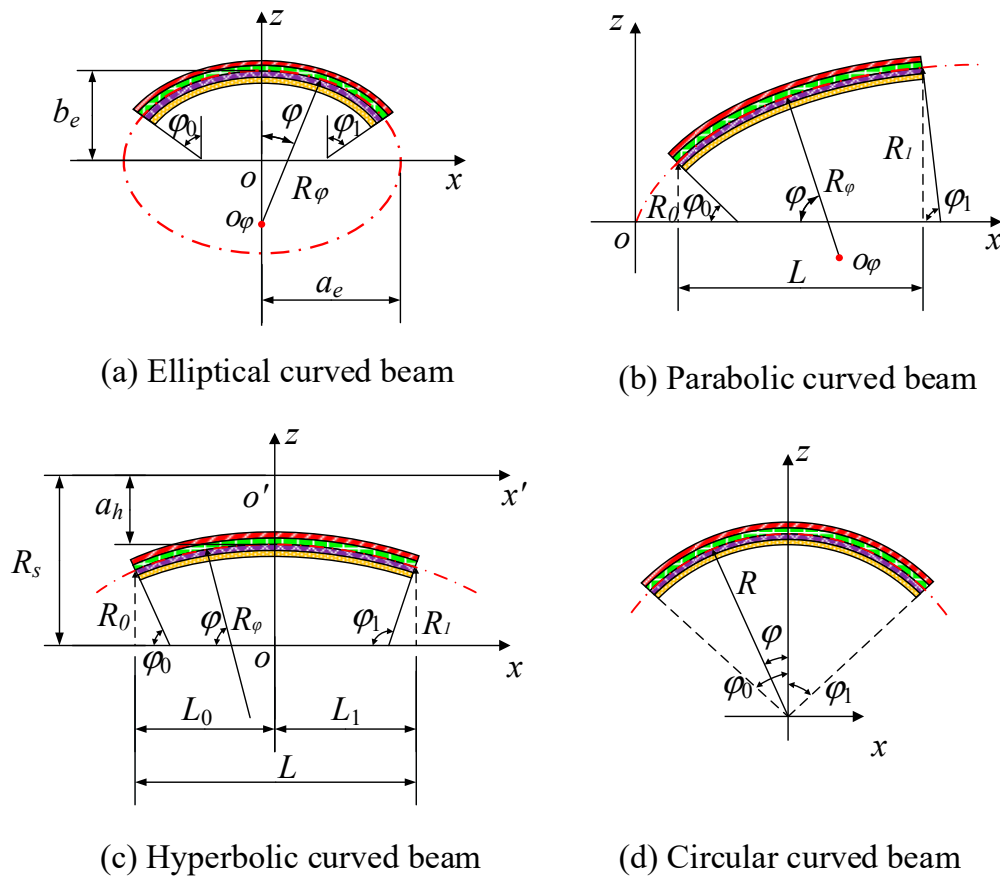


Figure 2. Different types of curved laminated composite beams (CLCBs): (a) Elliptic curved beam; (b) parabolic curved beam; (c) hyperbolic curved beam; (d) circular curved beam.

The hyperbolic CLCB (Figure 2c) is represented by the following equations:

$$R_\varphi(\varphi) = \frac{-a_h^2 b_h^2}{\sqrt{(a_h^2 \sin^2 \varphi - b_h^2 \cos^2 \varphi)^3}}, \tag{3a}$$

$$b_h = L_0 a_h / \sqrt{(R_0^2 - a_h^2)} = L_1 a_h / \sqrt{(R_1^2 - a_h^2)}, \tag{3b}$$

$$\varphi_0 = \arctan \left(\frac{(R_0 - R_s) b_h}{a_h \sqrt{(R_0 - R_s)^2 - a_h^2}} \right), \tag{3c}$$

$$\varphi_1 = \pi - \arctan \left(\frac{(R_1 - R_s) b_h}{a_h \sqrt{(R_1 - R_s)^2 - a_h^2}} \right), \tag{3d}$$

where R_s denotes the distance from ox to $o'x'$ (revolution axis); a_h signifies the length of the semitransverse axis, and b_h indicates that of the semiconjugate axis.

Figure 2d shows the circular curved beam, where R indicates the mean radius.

2.2. Energy Expression of the CLCB

The energy expressions of the CLCB are established in the framework of HSDT. Hence, the displacement components of the CLCB for an arbitrary point can be written as

$$\bar{U}(\varphi, y, z, t) = u(\varphi, y, t) + \psi_\varphi(\varphi, y, t)z + \phi_\varphi(\varphi, y, t)z^2 + \lambda_\varphi(\varphi, y, t)z^3, \tag{4a}$$

$$\bar{W}(\varphi, y, z, t) = w(\varphi, y, t), \tag{4b}$$

in which u and w indicate the displacements along the φ and z orientations at the middle surface, respectively. In addition, ψ_φ denotes the rotation of the transverse normal with respect to the φ direction. ϕ_φ and λ_φ signify the higher-order terms connected to the Taylor series. Mathematically,

$$\psi_\varphi = \left(\frac{\partial \bar{U}}{\partial z} \right)_{z=0}, \phi_\varphi = \frac{1}{2} \left(\frac{\partial^2 \bar{U}}{\partial z^2} \right)_{z=0}, \lambda_\varphi = \frac{1}{6} \left(\frac{\partial^3 \bar{U}}{\partial z^3} \right)_{z=0}. \tag{5}$$

The linear strain–displacement relationships, which consider z/R_φ terms, can be given as follows:

$$\varepsilon_\varphi = \frac{1}{1 + z/R_\varphi} (\varepsilon_\varphi^0 + zk_\varphi^0 + z^2 k_\varphi^1 + z^3 k_\varphi^2), \tag{6a}$$

$$\gamma_{\varphi z} = \frac{1}{1 + z/R_\varphi} (\gamma_{\varphi z}^0 + zk_{\varphi z}^0 + z^2 k_{\varphi z}^1 + z^3 k_{\varphi z}^2), \tag{6b}$$

where ε_φ^0 and $\gamma_{\varphi z}^0$ signify the middle surface normal and shear strains, respectively, and $k_\varphi^{i(i=0,1,2)}$ and $k_{\varphi z}^{i(i=0,1,2)}$ indicate curvature changes. They are defined as

$$\varepsilon_\varphi^0 = \frac{1}{R_\varphi} \left(\frac{\partial u}{\partial \varphi} + w \right), k_\varphi^0 = \frac{1}{R_\varphi} \frac{\partial \psi_\varphi}{\partial \varphi}, k_\varphi^1 = \frac{1}{R_\varphi} \frac{\partial \phi_\varphi}{\partial \varphi}, k_\varphi^2 = \frac{1}{R_\varphi} \frac{\partial \lambda_\varphi}{\partial \varphi}, \tag{7a}$$

$$\gamma_{\varphi z}^0 = \frac{1}{R_\varphi} \left(-u + \frac{\partial w}{\partial \varphi} \right) + \psi_\varphi, k_{\varphi z}^0 = 2\phi_\varphi, k_{\varphi z}^1 = \frac{1}{R_\varphi} \frac{\partial \phi_\varphi}{\partial \varphi} + 3\lambda_\varphi, k_{\varphi z}^2 = 2\frac{1}{R_\varphi} \lambda_\varphi. \tag{7b}$$

The force (N) and moment resultants (M) of the CLCB can be represented by middle surface strains and curvature changes:

$$\begin{pmatrix} N_\varphi \\ N_y \\ N_{\varphi y} \\ M_\varphi \\ M_y \\ M_{\varphi y} \\ N_\varphi^1 \\ N_y^1 \\ N_{\varphi y}^1 \\ M_\varphi^2 \\ M_y^2 \\ M_{\varphi y}^2 \end{pmatrix} = \begin{bmatrix} A_{11} & A_{12} & A_{16} & B_{11} & B_{12} & B_{16} & C_{11} & C_{12} & C_{16} & D_{11} & D_{12} & D_{16} \\ A_{12} & A_{22} & A_{26} & B_{12} & B_{22} & B_{26} & C_{12} & C_{22} & C_{26} & D_{12} & D_{22} & D_{26} \\ A_{16} & A_{26} & A_{66} & B_{16} & B_{26} & B_{66} & C_{16} & C_{26} & C_{66} & D_{16} & D_{26} & D_{66} \\ B_{11} & B_{12} & B_{16} & C_{11} & C_{12} & C_{16} & D_{11} & D_{12} & D_{16} & E_{11} & E_{12} & E_{16} \\ B_{12} & B_{22} & B_{26} & C_{12} & C_{22} & C_{26} & D_{12} & D_{22} & D_{26} & E_{12} & E_{22} & E_{26} \\ B_{16} & B_{26} & B_{66} & C_{16} & C_{26} & C_{66} & D_{16} & D_{26} & D_{66} & E_{16} & E_{26} & E_{66} \\ C_{11} & C_{12} & C_{16} & D_{11} & D_{12} & D_{16} & E_{11} & E_{12} & E_{16} & F_{11} & F_{12} & F_{16} \\ C_{12} & C_{22} & C_{26} & D_{12} & D_{22} & D_{26} & E_{12} & E_{22} & E_{26} & F_{12} & F_{22} & F_{26} \\ C_{16} & C_{26} & C_{66} & D_{16} & D_{26} & D_{66} & E_{16} & E_{26} & E_{66} & F_{16} & F_{26} & F_{66} \\ D_{11} & D_{12} & D_{16} & E_{11} & E_{12} & E_{16} & F_{11} & F_{12} & F_{16} & G_{11} & G_{12} & G_{16} \\ D_{12} & D_{22} & D_{26} & E_{12} & E_{22} & E_{26} & F_{12} & F_{22} & F_{26} & G_{12} & G_{22} & G_{26} \\ D_{16} & D_{26} & D_{66} & E_{16} & E_{26} & E_{66} & F_{16} & F_{26} & F_{66} & G_{16} & G_{26} & G_{66} \end{bmatrix} \begin{pmatrix} \varepsilon_\varphi^0 \\ \varepsilon_y^0 \\ \gamma_{\varphi y}^0 \\ k_\varphi^0 \\ k_y^0 \\ k_{\varphi y}^0 \\ k_\varphi^1 \\ k_y^1 \\ k_{\varphi y}^1 \\ k_\varphi^2 \\ k_y^2 \\ k_{\varphi y}^2 \end{pmatrix} \quad (8a)$$

$$\begin{pmatrix} Q_\varphi \\ Q_y \\ P_\varphi \\ P_y \\ Q_\varphi^1 \\ Q_y^1 \\ P_\varphi^2 \\ P_y^2 \end{pmatrix} = \begin{bmatrix} A_{55} & A_{45} & B_{55} & B_{45} & C_{55} & C_{45} & D_{55} & D_{45} \\ A_{45} & A_{44} & B_{45} & B_{44} & C_{45} & C_{44} & D_{45} & D_{44} \\ B_{55} & B_{45} & C_{55} & C_{45} & D_{55} & D_{45} & E_{55} & E_{45} \\ B_{45} & B_{44} & C_{45} & C_{44} & D_{45} & D_{44} & E_{45} & E_{44} \\ C_{55} & C_{45} & D_{55} & D_{45} & E_{55} & E_{45} & F_{55} & F_{45} \\ C_{45} & C_{44} & D_{45} & D_{44} & E_{45} & E_{44} & F_{45} & F_{44} \\ D_{55} & D_{45} & E_{55} & E_{45} & F_{55} & F_{45} & G_{55} & G_{45} \\ D_{45} & D_{44} & E_{45} & E_{44} & F_{45} & F_{44} & G_{45} & G_{44} \end{bmatrix} \begin{pmatrix} \gamma_{\varphi z}^0 \\ \gamma_{yz}^0 \\ k_{\varphi z}^0 \\ k_{yz}^0 \\ k_{\varphi z}^1 \\ k_{yz}^1 \\ k_{\varphi z}^2 \\ k_{yz}^2 \end{pmatrix} \quad (8b)$$

where N_φ , N_y , $N_{\varphi y}$, N_φ^1 , N_y^1 , and $N_{\varphi y}^1$ signify the in-plane forces; M_φ , M_y , $M_{\varphi y}$, M_φ^2 , M_y^2 , and $M_{\varphi y}^2$ denote the moment resultants; and Q_φ , Q_y , P_φ , P_y , Q_φ^1 , Q_y^1 , P_φ^2 , and P_y^2 indicate the transverse shear force resultants. The corresponding extensional stiffnesses A_{ij} ($i, j = 1, 2, 6$), coupling stiffnesses B_{ij} , bending stiffnesses C_{ij} , and other stiffness coefficients ($D_{ij}, E_{ij}, F_{ij}, G_{ij}$ and H_{ij}) can be expressed as

$$\{A_{ij}, B_{ij}, C_{ij}, D_{ij}, E_{ij}, F_{ij}, G_{ij}, H_{ij}\} = \sum_{k=1}^{N_k} \int_{z_k}^{z_{k+1}} \bar{S}_{ij}^k \{1, z, z^2, z^3, z^4, z^5, z^6, z^7\} dz, \quad (9)$$

where \bar{S}_{ij}^k indicates transformed reduced stiffness coefficients for the k 'th layer. In addition, they are defined as

$$\begin{aligned} \bar{S}_{11}^k &= S_{11}^k m^4 + 2(S_{12}^k + 2S_{66}^k) m^2 n^2 + S_{22}^k n^4, \\ \bar{S}_{12}^k &= (S_{11}^k + S_{22}^k - 4S_{66}^k) m^2 n^2 + S_{12}^k (m^4 + n^4), \\ \bar{S}_{22}^k &= S_{11}^k n^4 + 2(S_{12}^k + 2S_{66}^k) m^2 n^2 + S_{22}^k m^4, \\ \bar{S}_{16}^k &= (S_{11}^k - S_{12}^k - 2S_{66}^k) m^3 n + (S_{12}^k - S_{22}^k + 2S_{66}^k) mn^3, \\ \bar{S}_{26}^k &= (S_{11}^k - S_{12}^k - 2S_{66}^k) mn^3 + (S_{12}^k - S_{22}^k + 2S_{66}^k) m^3 n, \\ \bar{S}_{66}^k &= (S_{11}^k + S_{22}^k - 2S_{12}^k - 2S_{66}^k) m^2 n^2 + S_{66}^k (m^4 + n^4), \\ \bar{S}_{44}^k &= S_{44}^k m^2 + S_{55}^k n^2, \quad \bar{S}_{45}^k = (S_{55}^k - S_{44}^k) mn, \quad \bar{S}_{55}^k = S_{55}^k m^2 + S_{44}^k n^2, \\ S_{11}^k &= \frac{E_1^k}{1 - \mu_{12}^k \mu_{21}^k}, \quad S_{12}^k = \frac{\mu_{12}^k E_2^k}{1 - \mu_{12}^k \mu_{21}^k}, \quad S_{22}^k = \frac{E_2^k}{1 - \mu_{12}^k \mu_{21}^k}, \quad S_{44}^k = G_{23}^k, \quad S_{55}^k = G_{13}^k, \quad S_{66}^k = G_{12}^k, \\ m &= \cos \alpha_{fiber}^k, \quad n = \sin \alpha_{fiber}^k \end{aligned} \quad (10)$$

where α_{fiber}^k denotes the fiber orientation angle of the k 'th lamina with respect to the φ -axis of the CLCBs and S_{ef}^k ($e, f = 1, 2, 4, 5$, and 6) is the material properties. With regard to CLCBs, the following

parameters ($N_y, N_{\varphi y}, N_y^1$, and $N_{\varphi y}^1$; Q_y, P_y, Q_y^1 , and P_y^2 ; $M_y, M_{\varphi y}, M_y^2$, and $M_{\varphi y}^2$) are presumed to be zero. Hence, Equation (8) can be rewritten as

$$\begin{Bmatrix} N_\varphi \\ M_\varphi \\ N_\varphi^1 \\ M_\varphi^2 \end{Bmatrix} = \begin{bmatrix} \overline{A_{11}} & \overline{B_{11}} & \overline{C_{11}} & \overline{D_{11}} \\ \overline{B_{11}} & \overline{C_{11}} & \overline{D_{11}} & \overline{E_{11}} \\ \overline{C_{11}} & \overline{D_{11}} & \overline{E_{11}} & \overline{F_{11}} \\ \overline{D_{11}} & \overline{E_{11}} & \overline{F_{11}} & \overline{G_{11}} \end{bmatrix} \begin{Bmatrix} \varepsilon_\varphi^0 \\ k_\varphi^0 \\ k_\varphi^1 \\ k_\varphi^2 \end{Bmatrix} = \begin{bmatrix} \overline{A_{55}} & \overline{B_{55}} & \overline{C_{55}} & \overline{D_{55}} \\ \overline{B_{55}} & \overline{C_{55}} & \overline{D_{55}} & \overline{E_{55}} \\ \overline{C_{55}} & \overline{D_{55}} & \overline{E_{55}} & \overline{F_{55}} \\ \overline{D_{55}} & \overline{E_{55}} & \overline{F_{55}} & \overline{G_{55}} \end{bmatrix} \begin{Bmatrix} \gamma_{\varphi z}^0 \\ k_{\varphi z}^0 \\ k_{\varphi z}^1 \\ k_{\varphi z}^2 \end{Bmatrix}, \quad (11)$$

where

$$\overline{A_{ij}} = \overline{\overline{A_{ij}}} - 1/R_\varphi \overline{\overline{B_{ij}}}, \quad \overline{B_{ij}} = \overline{\overline{B_{ij}}} - 1/R_\varphi \overline{\overline{C_{ij}}}, \quad \overline{C_{ij}} = \overline{\overline{C_{ij}}} - 1/R_\varphi \overline{\overline{D_{ij}}}, \quad (12a)$$

$$\overline{D_{ij}} = \overline{\overline{D_{ij}}} - 1/R_\varphi \overline{\overline{E_{ij}}}, \quad \overline{E_{ij}} = \overline{\overline{E_{ij}}} - 1/R_\varphi \overline{\overline{F_{ij}}}, \quad \overline{F_{ij}} = \overline{\overline{F_{ij}}} - 1/R_\varphi \overline{\overline{G_{ij}}}, \quad \overline{G_{ij}} = \overline{\overline{G_{ij}}} - 1/R_\varphi \overline{H_{ij}}, \quad (12b)$$

$$\overline{\overline{\mathbf{A}}} = \mathbf{A} - \mathbf{BC}^{-1}\mathbf{B}^T, \quad (12c)$$

$$\overline{\overline{\mathbf{A}}} = \begin{bmatrix} \overline{\overline{A_{11}}} & \overline{\overline{B_{11}}} & \overline{\overline{C_{11}}} & \overline{\overline{D_{11}}} \\ \overline{\overline{B_{11}}} & \overline{\overline{C_{11}}} & \overline{\overline{D_{11}}} & \overline{\overline{E_{11}}} \\ \overline{\overline{C_{11}}} & \overline{\overline{D_{11}}} & \overline{\overline{E_{11}}} & \overline{\overline{F_{11}}} \\ \overline{\overline{D_{11}}} & \overline{\overline{E_{11}}} & \overline{\overline{F_{11}}} & \overline{\overline{G_{11}}} \end{bmatrix} \mathbf{A} = \begin{bmatrix} A_{11} & B_{11} & C_{11} & D_{11} \\ B_{11} & C_{11} & D_{11} & E_{11} \\ C_{11} & D_{11} & E_{11} & F_{11} \\ D_{11} & E_{11} & F_{11} & G_{11} \end{bmatrix}, \quad (12d)$$

$$\mathbf{B} = \begin{bmatrix} A_{12} & A_{16} & B_{12} & B_{16} & C_{12} & C_{16} & D_{12} & D_{16} \\ B_{12} & B_{16} & C_{12} & C_{16} & D_{12} & D_{16} & E_{12} & E_{16} \\ C_{12} & C_{16} & D_{12} & D_{16} & E_{12} & E_{16} & F_{12} & F_{16} \\ D_{12} & D_{16} & E_{12} & E_{16} & F_{12} & F_{16} & G_{12} & G_{16} \end{bmatrix}, \quad (12e)$$

$$\mathbf{C} = \begin{bmatrix} A_{22} & A_{26} & B_{22} & B_{26} & C_{22} & C_{26} & D_{22} & D_{26} \\ A_{26} & A_{66} & B_{26} & B_{66} & C_{26} & C_{66} & D_{26} & D_{66} \\ B_{22} & B_{26} & C_{22} & C_{26} & D_{22} & D_{26} & E_{22} & E_{26} \\ B_{26} & B_{66} & C_{26} & C_{66} & D_{26} & D_{66} & E_{26} & E_{66} \\ C_{22} & C_{26} & D_{22} & D_{26} & E_{22} & E_{26} & F_{22} & F_{26} \\ C_{26} & C_{66} & D_{26} & D_{66} & E_{26} & E_{66} & F_{26} & F_{66} \\ D_{22} & D_{26} & E_{22} & E_{26} & F_{22} & F_{26} & G_{22} & G_{26} \\ D_{26} & D_{66} & E_{26} & E_{66} & F_{26} & F_{66} & G_{26} & G_{66} \end{bmatrix}, \quad (12f)$$

$$\overline{\overline{\mathbf{Q}}} = \mathbf{Q} - \mathbf{SP}^{-1}\mathbf{S}^T, \quad (12g)$$

$$\overline{\overline{\mathbf{Q}}} = \begin{bmatrix} \overline{\overline{A_{55}}} & \overline{\overline{B_{55}}} & \overline{\overline{C_{55}}} & \overline{\overline{D_{55}}} \\ \overline{\overline{B_{55}}} & \overline{\overline{C_{55}}} & \overline{\overline{D_{55}}} & \overline{\overline{E_{55}}} \\ \overline{\overline{C_{55}}} & \overline{\overline{D_{55}}} & \overline{\overline{E_{55}}} & \overline{\overline{F_{55}}} \\ \overline{\overline{D_{55}}} & \overline{\overline{E_{55}}} & \overline{\overline{F_{55}}} & \overline{\overline{G_{55}}} \end{bmatrix} \mathbf{Q} = \begin{bmatrix} A_{55} & B_{55} & C_{55} & D_{55} \\ B_{55} & C_{55} & D_{55} & E_{55} \\ C_{55} & D_{55} & E_{55} & F_{55} \\ D_{55} & E_{55} & F_{55} & G_{55} \end{bmatrix}, \quad (12h)$$

$$\mathbf{S} = \begin{bmatrix} A_{45} & B_{45} & C_{45} & D_{45} \\ B_{45} & C_{45} & D_{45} & E_{45} \\ C_{45} & D_{45} & E_{45} & F_{45} \\ D_{45} & E_{45} & F_{45} & G_{45} \end{bmatrix} \mathbf{P} = \begin{bmatrix} A_{44} & B_{44} & C_{44} & D_{44} \\ B_{44} & C_{44} & D_{44} & E_{44} \\ C_{44} & D_{44} & E_{44} & F_{44} \\ D_{44} & E_{44} & F_{44} & G_{44} \end{bmatrix}. \quad (12i)$$

On the foundation of previous discussions, the kinetic energy of the CLCB may be represented as

$$\begin{aligned}
 T &= \frac{1}{2} \iiint_V \rho(z) \left[\left(\dot{\bar{U}}_{ij} \right)^2 + \left(\dot{\bar{W}}_{ij} \right)^2 \right] \left(1 + \frac{z}{R_\varphi} \right) R_\varphi d\varphi dy dz = \\
 &= \frac{1}{2} b \int_{\varphi_0}^{\varphi_1} \left\{ I_0 \left[\left(\dot{u} \right)^2 + \left(\dot{w} \right)^2 \right] + 2I_1 \dot{u} \dot{\psi}_\varphi + I_2 \left(\dot{\psi}_\varphi^2 + 2\dot{u} \dot{\phi}_\varphi \right) \right. \\
 &\quad \left. + 2I_3 \left(\dot{u} \dot{\lambda}_\varphi + \dot{\psi}_\varphi \dot{\phi}_\varphi \right) + I_4 \left(\dot{\phi}_\varphi^2 + 2\dot{\psi}_\varphi \dot{\lambda}_\varphi \right) + 2I_5 \dot{\phi}_\varphi \dot{\lambda}_\varphi + I_6 \dot{\lambda}_\varphi^2 \right\} R_\varphi d\varphi
 \end{aligned} \quad (13)$$

where

$$(I_0, I_1, I_2, I_3, I_4, I_5, I_6) = \int_{z_k}^{z_{k+1}} \rho(z) \left(1 + \frac{z}{R_\varphi} \right) (1, z, z^2, z^3, z^4, z^5, z^6) dz. \quad (14)$$

Besides, the strain energy may be expressed as

$$U = \frac{1}{2} \iiint_V \left(N_\varphi \varepsilon_\varphi^0 + M_\varphi k_\varphi^0 + N_\varphi^1 k_\varphi^1 + M_\varphi^2 k_\varphi^2 + Q_\varphi \gamma_{\varphi z}^0 + P_\varphi k_{\varphi z}^0 + Q_\varphi^1 k_{\varphi z}^1 + P_\varphi^2 k_{\varphi z}^2 \right) R_\varphi d\varphi dy dz. \quad (15)$$

2.3. Variational Formulation for Curved Beam

In general, by solving the governing equations associated with boundary conditions, the eigenvalue solutions can be gained. However, it is not an easy job to conduct this process, as choosing suitable admissible functions for arbitrary boundary conditions is difficult. Alternatively, a new procedure by which the problem is expressed in a modified variational form may be developed to simplify the solution.

In this research, a highly efficient and accurate variational approach is adopted and vibration analysis of moderately tall CLCBs with diverse curvatures is conducted. First, the total variational functional Π_{total} is obtained, the terms of which include the kinetic energy T , strain energy U , and strain energy function connected with the interface and boundary restraint Π_{pf} . Then, the displacement field is expanded in terms of Jacobi polynomials, which contain unknown Jacobi expanded coefficients. By conducting the variational operation (i.e., $\delta \Pi_{total} = 0$) with respect to unknown Jacobi expanded coefficients, an equation in matrix form can be acquired. Through solving this equation, the frequencies and corresponding mode shapes can be easily determined.

Besides, the formulation is derived by employing the multi-segment partitioning technique. The curved beam is separated into N_φ identical segments along the φ orientation. As each segment becomes a free–free substructure, the displacement discretization with respect to admissible functions becomes more convenient. This is related to the fact that the continuity conditions of the CLCB need not be imposed, as their satisfaction is implemented in a variational statement. As such, the issue is simplified to simulating the interaction of each beam segment with common boundaries. This will make the computer implementation of CLCBs much simpler: (a) The selections of admissible functions become flexible as both boundary and continuity conditions are relaxed; (b) by flexibly choosing the appropriate admissible functions, the convergence performance of the present methodology can be quite fast and stable; and (c) the accuracy of the modified variational method can be substantially improved by segmentation, especially for higher modes. Then, the vibration problem may be distinguished by an improved variational principle [24–26], which turns into finding the minimum value of a variational functional as

$$\prod_{ve} = \sum_{i=1}^{N_\varphi} (U_i - T_i), \quad (16)$$

where T_i is the maximum kinetic energy of the i 'th beam segment and U_i is the corresponding maximum strain energy.

To construct a uniform model to handle arbitrary boundary conditions, as well as ensure numerical stability, the technique of penalty function is exploited. The strain energy function connected with the boundary elastic restraint can be shown as

$$\begin{aligned}
 \Pi_{pf} &= \frac{1}{2} \sum_{i=1}^{N_\varphi} \left[\eta_u k_u (u_i - u_{i+1})^2 + \eta_w k_w (w_i - w_{i+1})^2 + \eta_\varphi k_\varphi (\varphi_i - \varphi_{i+1})^2 \right. \\
 &\quad \left. + \eta_\phi k_\phi (\phi_i - \phi_{i+1})^2 + \eta_v k_v (v_i - v_{i+1})^2 \right] \\
 &= \frac{1}{2} \left[k_{u0} u^2 + k_{w0} w^2 + k_{\varphi 0} \varphi^2 + k_{\phi 0} \phi^2 + k_{v0} v^2 \right]_{\varphi=\varphi_0} \\
 &\quad + \frac{1}{2} \left[k_{u1} u^2 + k_{w1} w^2 + k_{\varphi 1} \varphi^2 + k_{\phi 1} \phi^2 + k_{v1} v^2 \right]_{\varphi=\varphi_1} \\
 &\quad + \frac{1}{2} \sum_{i=1}^{N_\varphi} \left[k_u (u_i - u_{i+1})^2 + k_w (w_i - w_{i+1})^2 + k_\varphi (\varphi_i - \varphi_{i+1})^2 \right. \\
 &\quad \left. + k_\phi (\phi_i - \phi_{i+1})^2 + k_v (v_i - v_{i+1})^2 \right]
 \end{aligned} \tag{17}$$

where $k_\tau (\tau = u, w, \varphi, \phi, v)$ indicates the penalty terms expressing the elastic stiffness at both ends of the curved beam, and $\eta_\tau (\tau = u, w, \varphi, \phi, v)$ represents the continuity or boundary coefficients. By properly defining η_τ and k_τ , both continuity conditions for the interface and the arbitrary boundary conditions can be conveniently obtained. For the continuity conditions of two neighbored curved beam domains, the continuity coefficients $\eta_\tau (\tau = u, w, \varphi, \phi, v) = 1$, while for boundary conditions, different combinations of boundary coefficients η_τ and k_τ are imposed to achieve various boundary conditions (Table 1). Meanwhile, it is worth noting that both classical and elastic boundary restraints can be achieved by properly selecting the values of $k_\tau (\tau = u, w, \varphi, \phi, v)$; note that $k_{\tau 0}$ and $k_{\tau 1}$ represent the penalty terms at edges $\varphi = \varphi_0$ and $\varphi = \varphi_1$, respectively. The elastic boundary restraints represent a boundary condition between simply supported and clamped boundary conditions, which can be modeled by springs at the edges. For instance, by setting one or some of the $k_\tau (\tau = u, w, \varphi, \phi, v)$ at certain values, the elastic boundary conditions can be conveniently obtained.

Table 1. Boundary coefficients and penalty parameters for various boundary conditions.

Boundary Conditions	Boundary Coefficients					Penalty Parameters				
	η_u	η_w	η_φ	η_ϕ	η_v	k_u	k_w	k_φ	k_ϕ	k_v
Free (F)	0	0	0	0	0	0	0	0	0	0
Simply supported (SS)	1	1	0	0	0	10^{14}	10^{14}	0	0	0
Slided (SD)	0	1	0	0	0	0	10^{14}	0	0	0
Clamped (C)	1	1	1	1	1	10^{14}	10^{14}	10^{14}	10^8	10^8
Elastic supported 1 (E1)	1	1	1	1	1	10^8	10^8	10^{14}	10^8	10^8
Elastic supported 1 (E2)	1	1	1	1	1	10^{14}	10^{14}	10^8	10^8	10^8
Elastic supported 1 (E3)	1	1	1	1	1	10^8	10^8	10^8	10^8	10^8

More information about the penalty terms to handle the boundary conditions can be found in previous investigations [27–31]. Consequently, the variational form for a CLCB subjected to arbitrary boundary conditions is

$$\prod_{total} = \sum_{i=1}^{N_\varphi} (U_i - T_i) + \prod_{pf} \tag{18}$$

2.4. Solution Procedure

By introducing the modified variational approach in conjunction with the multi-segment partitioning strategy, the choice of admissible displacements for each beam segment can be flexible. This is due to the fact that continuity and boundary conditions of the curved beam are relaxed by the functional \prod_{total} . The \prod_{total} allows the use of identical displacement functions for every curved beam

segment. In the present analysis, the displacement components for each divided segment of the CLCB are congruously represented by means of Jacobi polynomials.

$$u^i = \sum_{m=0}^M U_m P_m^{(\alpha,\beta)}(\varphi) e^{i\omega t}, \quad (19a)$$

$$w^i = \sum_{m=0}^M W_m P_m^{(\alpha,\beta)}(\varphi) e^{i\omega t}, \quad (19b)$$

$$\psi_{\varphi}^i = \sum_{m=0}^M \psi_{\varphi_m} P_m^{(\alpha,\beta)}(\varphi) e^{i\omega t}, \quad (19c)$$

$$\phi_{\varphi}^i = \sum_{m=0}^M \Phi_{\varphi_m} P_m^{(\alpha,\beta)}(\varphi) e^{i\omega t}, \quad (19d)$$

$$\lambda_{\varphi}^i = \sum_{m=0}^M \Upsilon_{\varphi_m} P_m^{(\alpha,\beta)}(\varphi) e^{i\omega t}, \quad (19e)$$

where U_m , W_m , ψ_{φ_m} , Φ_{φ_m} , and Υ_{φ_m} indicate the relevant Jacobi expanded coefficients; $P_m^{(\alpha,\beta)}(\varphi)$ represents the Jacobi polynomial of order m , which is related to the displacement components along the central line orientation; and ω and t signify angular frequency and time, respectively. Besides, the maximum value of m or the truncation terms are represented by M . By choosing different combinations of Jacobi parameters α and β , various orthogonal polynomials can be obtained such as Chebyshev, Gegenbauer, and Legendre polynomials. More details about these can be discovered in [32–34]. Substituting Equations (13) and (15)–(17) into Equation (18) and incorporating Equation (19), the following can be achieved:

$$\prod_{total} = \prod_{total} (U_m, V_m, \psi_{\varphi_m}, \Phi_{\varphi_m}, \Upsilon_{\varphi_m}). \quad (20)$$

Conducting the variation operation for \prod_{total} , i.e., $\delta \prod_{total} = 0$, with regard to Jacobi expanded coefficients (U_m , V_m , ψ_{φ_m} , Φ_{φ_m} , and Υ_{φ_m}), the following characteristic equations can be obtained:

$$(\mathbf{K} - \omega^2 \mathbf{M})\mathbf{E} = 0, \quad (21)$$

in which \mathbf{K} signifies the stiffness matrix, \mathbf{M} indicates the mass matrix, and \mathbf{E} denotes the undetermined coefficients. Apparently, through the solution of Equation (21), the eigenvalues and eigenvectors can be acquired.

3. Results and Discussions

In this part, the convergence performance, reliability, efficiency, and accuracy of the current methodology are studied by a number of numerical cases. For the sake of brevity, the free, clamped, simply supported, slided, and elastic boundary conditions are represented by F, C, SS, SD, and E, respectively, as shown in Table 1. Besides, three kinds of elastic boundary restraints (E1, E2, and E3) are taken into consideration. Then, a two-letter string is utilized to represent the boundary conditions of two ends, e.g., SS-E indicates the curved beam subjected to the simply supported boundary condition at edge $\varphi = \varphi_0$ and the elastic one at edge $\varphi = \varphi_1$.

First, it is essential to investigate the convergence performance of the present modified variational approach for vibration analysis of the curved beam. To begin with, the comparison of dimensionless frequencies Ω for a C-C circular CLCB with respect to different N_{φ} is presented in Table 2. The non-dimensional frequency Ω is defined as $\Omega = \omega(R^2(\varphi_1 - \varphi_0)^2) \sqrt{12\rho/(E_1 h^2)}$. Two thicknesses h

= 0.1 and 0.2 m are considered. The material properties are $\rho = 1580 \text{ kg/m}^3$, $E_2 = 10 \text{ GPa}$, $E_1 = 15E_2$, $G_{12} = G_{13} = G_{23} = 0.55E_2$, $\mu_{12} = 0.27$, and $[\alpha_{fiber}^1 / \alpha_{fiber}^2] = [0^\circ / 90^\circ]$ (i.e., the fiber orientation angles of the first and second lamina are 0° and 90° , respectively). In addition, the geometric parameters are $\varphi_0 = -\pi/3$ and $\varphi_1 = \pi/3$. The Jacobi parameters are $\alpha = \beta = 0$ and the truncation number is $M = 8$. The number of segments is selected as $N_\varphi = 2, 4, 6, 8$, and 10 . In addition, the results from exact solutions exploiting CBT [3] and exact serious results based on FSDT [14] are shown for comparison. As N_φ is increased, fast convergence of Ω can be observed. In addition, the present results coincide well with the ones by FSDT and CBT. As a consequence, with small N_φ , accurate results of Ω can be achieved. For subsequent cases, unless otherwise specified, $N_\varphi = 8$ is chosen by default.

Table 2. Comparison of dimensionless frequencies Ω (first five modes) for a C-C curved laminated composite beam with respect to different N_φ .

h	Mode Number	Number of the Segment N_φ					Ref. [14]	Ref. [3]
		2	4	6	8	10		
0.1	1	23.519	23.514	23.514	23.513	23.513	23.245	23.628
	2	43.556	43.540	43.537	43.538	43.536	42.803	43.800
	3	76.148	76.105	76.101	76.099	76.099	74.476	76.687
	4	94.982	94.936	94.929	94.925	94.921	93.286	95.388
	5	122.318	122.192	122.186	122.183	122.180	120.064	123.059
0.2	1	19.816	19.805	19.803	19.799	19.795	19.116	20.005
	2	32.761	32.736	32.724	32.714	32.703	31.450	33.003
	3	55.356	55.340	55.304	55.264	55.224	52.850	55.849
	4	55.495	55.480	55.454	55.446	55.437	54.094	55.971
	5	79.636	79.568	79.550	79.544	79.533	75.675	80.422

Secondly, the influence of penalty terms k_τ ($\tau = u, w, \varphi, \phi, v$) (see Equation (19)) on Ω is investigated. The dimensionless frequency Ω versus penalty parameters k_t for a C-C curved beam is shown in Figure 3. The free vibration of CLCBs with arbitrary boundary conditions including both classical (clamped, free, and simply supported boundary conditions) and elastic boundary conditions is investigated. Here, for the convergence performance of penalty terms, the typical C-C boundary conditions are selected. Note that for other boundary conditions, similar results can be achieved. The material properties, geometric parameters, Jacobi parameters (α and β), and number of truncation terms M are the same as those of Table 2. For each case, one type of k_τ is varied from 10^0 to 10^{16} while the others are unchanged ($= 10^{14}$). When penalty parameters are absent or small, pseudo-rigid modes might emerge, indicating that the continuity conditions of the interface may not be imposed properly. By augmenting k_τ , the continuity condition can be satisfied. It is observed that when k_τ is in the range of 10^{10} – 10^{16} , the solution becomes very stable, with Ω remaining the same. Therefore, $k_{\tau(u,v,\varphi)} = 10^{14}$ and $k_{\tau(\phi,v)} = 10^{12}$ are employed as the coupling parameters in the following discussions. It should be noted that for different types of curved beams (e.g., elliptical, paraboloidal, and hyperbolical ones), when $k_{\tau(u,v,\varphi)} > 10^{10}$ and $k_{\tau(\phi,v)} > 10^8$, similarly, Ω converges to certain values (not shown). Thus, the determinations of penalty and boundary parameters are consistent for different curved beams.

It has been mentioned before that the present approach can be applicable to the prediction of the vibration behavior of a curved laminated beam subjected to elastic boundary conditions. Hence, the impact of boundary parameters on the vibration characteristics should be analyzed. The dimensionless frequency Ω versus boundary parameters k_τ for a C-E curved laminated beam is shown in Figure 4, with the other parameters being the same as those of Figure 3. The edge $\varphi = \varphi_0$ is clamped while the border $\varphi = \varphi_1$ is elastically supported. For the edge $\varphi = \varphi_1$, one set of boundary springs vary between 10^0 and 10^{16} while the others are presumed to be infinity ($= 10^{14}$). The variations of Ω with k_τ are similar to those in Figure 3, and the results can reflect that the determination of k_τ in Table 1 for different boundary conditions should be appropriate.

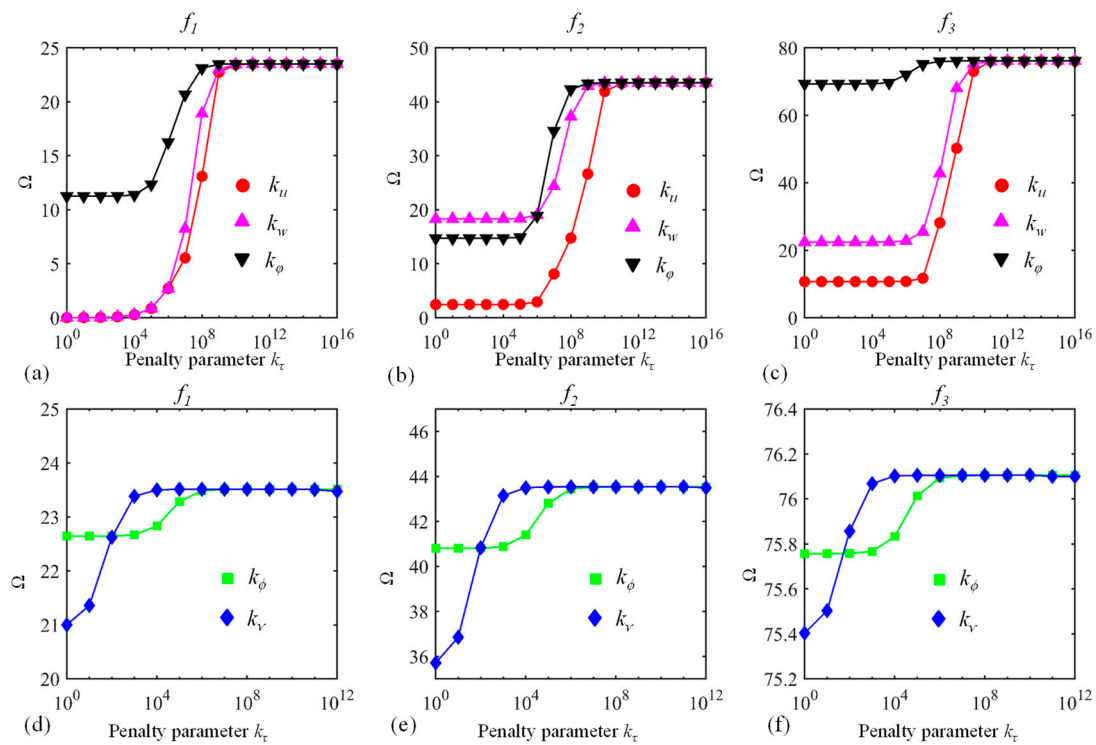


Figure 3. Dimensionless frequency Ω versus penalty parameters k_τ : (a–c) k_τ ($\tau = u, w, \phi$) and (d–f) k_τ ($\tau = \phi, \nu$). The first three modes (f_1, f_2 , and f_3) are considered.

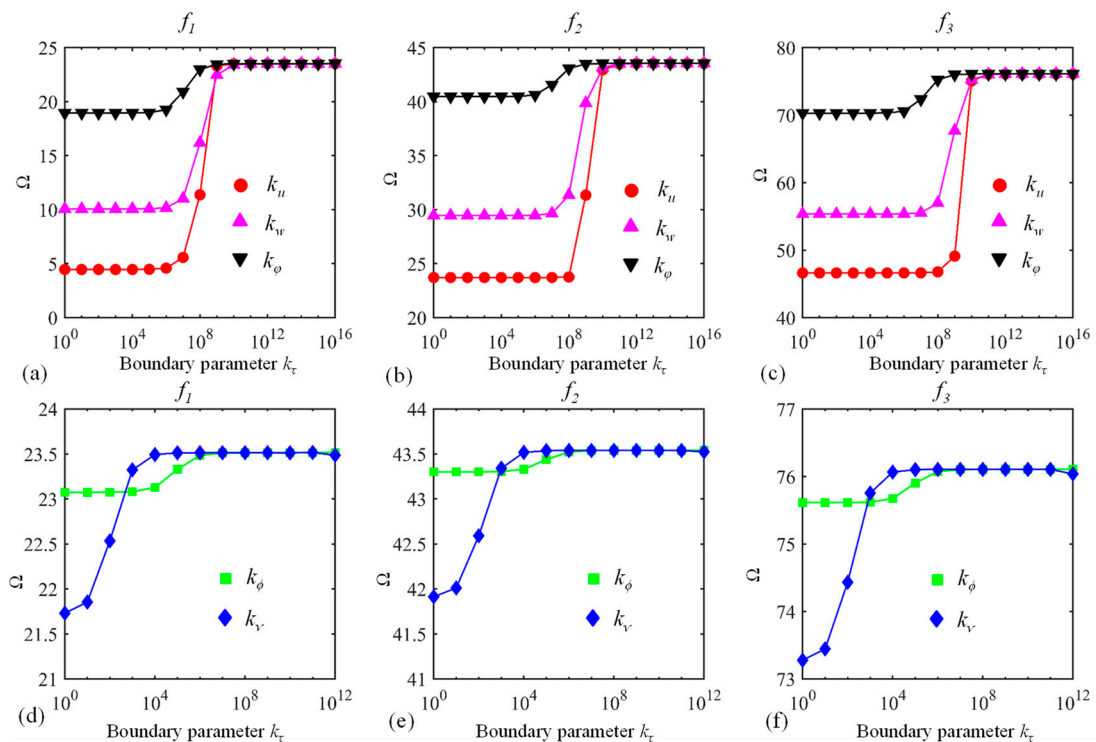


Figure 4. Dimensionless frequency Ω versus boundary parameters k_τ : (a–c) k_τ ($\tau = u, w, \phi$) and (d–f) k_τ ($\tau = \phi, \nu$). The first three modes (f_1, f_2 , and f_3) are considered.

Thirdly, the Jacobi orthogonal polynomials including the number of truncation terms and Jacobi parameters (α and β) should be investigated. The dimensionless frequency Ω versus truncation terms M for a circular CLCB and elliptical CLCB with the C-C boundary condition is displayed in Figure 5a,b,

respectively, the other parameters remaining the same as those of Figure 3. Obviously, for both cases, Ω converges very fast with the increase in M . As M becomes larger than 8, Ω (first five modes) converges to certain values. Subsequently, $M = 8$ is selected for all the numerical examples. To demonstrate the effect of Jacobi parameters (α and β) on the vibration behavior of the curved beam, the percentage error of Ω for various combinations of α and β is illustrated in Figure 6. Several combinations of (α, β) including $(\alpha, \beta) = (-0.5, -0.5), (-0.5, 0), (0.5, 0), (0, 0.5), (0.5, 0.5),$ and $(1, 1)$ are chosen. The results of $(\alpha, \beta) = (0, 0)$ are used as the base results, with the percentage error defined as $(\Omega_{\alpha,\beta} - \Omega_{\alpha=0,\beta=0}) / \Omega_{\alpha=0,\beta=0}$. In addition, three types of boundary restraints are considered: F-F, F-C, and C-C boundary conditions. It is shown that the maximum value of the percentage error is no more than 2×10^{-2} , which may indicate that the Jacobi parameters may not affect the value of Ω . Thus, different admissible displacement functions with various Jacobi parameters can be used to establish the formulation, leading to flexible selections of admissible displacements. For the following calculations, unless otherwise stated, $(\alpha, \beta) = (0, 0)$ is utilized.

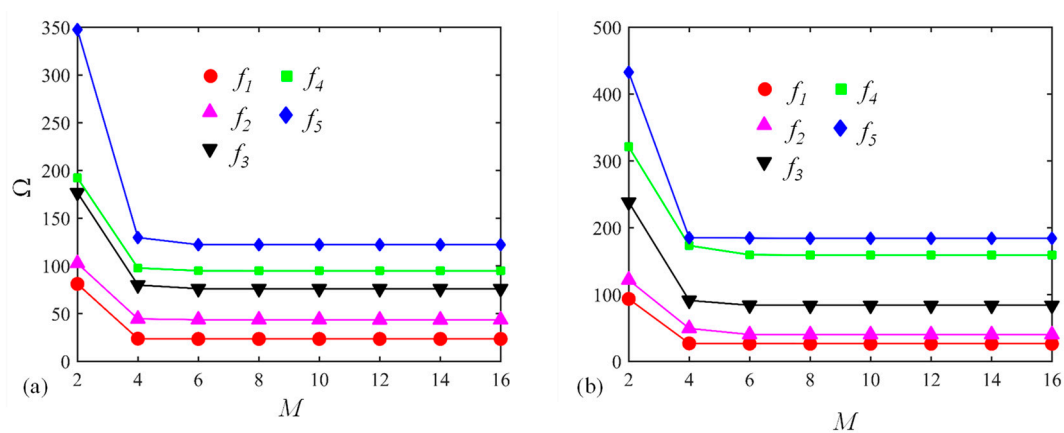


Figure 5. Dimensionless frequency Ω versus truncation terms M for (a) a circular CLCB and (b) an elliptical CLCB with C-C boundary condition.

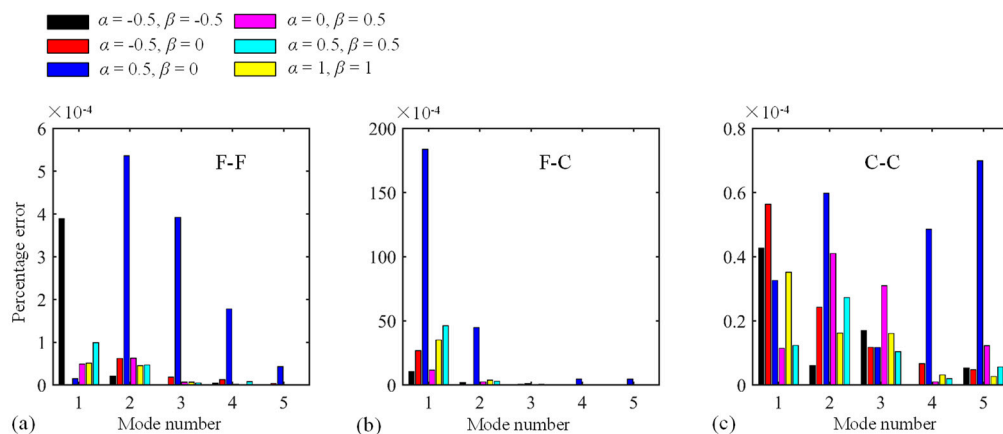


Figure 6. Percentage error of Ω for diverse combinations of α and β . (a) F-F boundary condition; (b) F-C boundary condition; (c) C-C boundary condition

After comprehending the characteristics of several parameters, it is necessary to show the reliability and precision of the present approach. Due to lack of experimental data, the present results are compared to those from results by other numerical studies in the literature. To further validate the present method, the finite element method (FEM) is also utilized for comparison. Table 3 shows the comparison of Ω (first eight modes) for the C-C elliptical, paraboloidal, and hyperbolical CLCBs. The material parameters are $\rho = 1500 \text{ kg/m}^3, E_2 = 10 \text{ GPa}, E_1 = 15E_2, G_{12} = G_{13} = 0.5E_2, G_{23} = 0.6E_2, \mu_{12} = 0.25,$ and $\alpha_{fiber}^k = [0^\circ/90^\circ/0^\circ]$. The geometric dimensions are: (a) **Elliptical one:** $h = 0.15 \text{ m},$

$a_e = 2$ m, $b_e = 1$ m, $\varphi_0 = 0$, and $\varphi_1 = \pi/2$; (b) **Paraboloidal one:** $h = 0.15$ m, $L = 1$ m, $R_0 = 0.2$ m, and $R_1 = 1$ m; **Hyperbolical one:** $a_h = 3$ m, $h = 0.15$ m, $R_0 = 0.2$ m, $R_1 = 1$ m, $R_s = 4$ m, and $L = 1$ m. Free vibration results obtained through the finite element method (FEM) using ABAQUS software are given as a reference. The types of elements are quadrilateral S4R (S4R is a general shell element type in ABAQUS) for all the cases. The numbers of elements for the elliptical, paraboloidal, and hyperbolical beams are 5808, 1310, and 1330, respectively. As shown in Table 3, the errors of the results by the present method and those by the FEM are not larger than 2.92%, which is small and indicates the accuracy of the present methodology. The natural frequencies depend on the different radii of curvature, lamination schemes, and boundary conditions. The differences of frequencies at the C-C boundary condition with respect to different types of CLCB (i.e., elliptical, paraboloidal, and hyperbolical) should be related to the radii of curvature changes. Then, the comparison of Ω for circular CLCBs subjected to various boundary conditions is displayed in Table 4. Results from the decomposition approach [17] and wave solution method [35] are given as a contrast. Three boundary restraints F-F, F-C, and C-SS are taken into account. For all the cases, the frequencies are in complete agreement. To further validate the present method, several mode shapes for curved composite laminated beams including elliptical, paraboloidal, and hyperbolical ones in the x - z plane are presented in Figure 7. The mode shapes obtained by the FEM through ABAQUS are presented for comparison. Apparently, all the mode shapes from the present methodology and FEM match well with each other. On the whole, the present methodology is capable of solving the vibration problem of the CLCB subjected to arbitrary boundary conditions.

Table 3. Comparison of frequencies (first eight modes) for C-C elliptical, paraboloidal, and hyperbolical curved laminated composite beams.

Mode No.	Elliptical Beam			Paraboloidal Beam			Hyperbolical Beam		
	Present	FEM	Error (%)	Present	FEM	Error (%)	Present	FEM	Error (%)
1	380.16	376.6	0.95	739.05	734	0.68	793.17	784.9	1.05
2	594.22	589.8	0.75	1162.5	1155.3	0.62	1207.4	1195.3	1.01
3	934.78	930.1	0.50	1826.5	1807.7	1.03	1809.0	1773.4	2.01
4	1116.0	1111.4	0.41	2481.2	2449.6	1.27	2433.8	2375.3	2.46
5	1503.5	1490.6	0.87	3161.2	3110.7	1.60	3107.4	3042	2.15
6	1819.4	1813.8	0.31	3409.7	3391	0.55	3451.1	3443.1	0.23
7	2169.6	2151.3	0.85	4011.5	3915.2	2.40	3979.0	3866	2.92
8	2375.5	2359.8	0.67	4655.6	4582	1.58	4565.8	4498.2	1.50

Finally, several novel results are presented, which can be served as benchmark solutions. The frequencies (first five modes) for the elliptical, paraboloidal, and hyperbolical CLCB with diverse lamination schemes and boundary conditions are shown in Tables 5–7, respectively. For each kind of beam, four lamination schemes including $\alpha_{fiber}^k = [0^\circ]$, $[0^\circ/90^\circ]$, $[0^\circ/90^\circ/0^\circ]$, and $[0^\circ/90^\circ/0^\circ/90^\circ]$ are considered. Besides, four types of classical (C-C, SS-SD, F-C, and F-F) and three kinds of elastic boundary restraints (E1-E1, E2-E2, and E3-E3) are studied. The geometric parameters are: (a) **Elliptical one:** $h = 0.2$ m, $b_e = 1$ m, $a_e = 2$ m, $\varphi_0 = -\pi/3$, and $\varphi_1 = \pi/3$; (b) **Paraboloidal one:** $h = 0.2$ m, $L = 2$ m, $R_0 = 0.2$ m, and $R_1 = 1$ m; and (c) **Hyperbolical one:** $h = 0.2$ m, $a_h = 3$ m, $R_s = 4$ m, $R_0 = 0.5$ m, $R_1 = 0.5$ m, $L = 2$ m, and $L_1 = 1$ m. Several aspects should be pointed out in Tables 5–7. First, the natural frequencies depend on the different radii of curvature, lamination schemes, and boundary conditions. Secondly, despite different radii of curvature and boundary conditions, the fundamental frequencies of the CLCB that own a single layer ($[0^\circ]$) or symmetric lamination $[0^\circ/90^\circ/0^\circ]$ are always those that have anti-symmetric laminations ($[0^\circ/90^\circ]$ and $[0^\circ/90^\circ/0^\circ/90^\circ]$). Thirdly, the C-C boundary condition always corresponds to the largest fundamental frequencies, regardless of the radii of curvature and lamination schemes.

Table 4. Comparison of Ω (first five modes) for circular curved laminated beams subjected to various boundary conditions.

Mode No.	F-F			F-C			C-SS		
	HBT _[LST]	HBT _[LMR]	Present	HBT _[LST]	HBT _[LMR]	Present	HBT _[LST]	HBT _[LMR]	Present
1	765.68	765.306	771.373	338.33	338.197	343.494	764.78	763.348	769.884
2	2100.96	2097.346	2115.244	1349.00	1346.992	1341.057	2097.01	2088.465	2108.493
3	4092.08	4077.308	4115.793	3019.38	3009.457	3093.753	4081.73	4053.791	4097.477
4	6707.87	6666.978	6744.373	5329.25	5298.837	5384.977	6686.94	6619.074	6700.256

Table 5. Frequencies (first five modes) for an elliptical curved laminated composite beam with diverse lamination schemes and boundary conditions.

Lamination Schemes (°)	f (Hz)	Boundary Conditions						
		F-F	F-C	SS-SD	C-C	E1-E1	E2-E2	E3-E3
[0]	1	103.35	18.207	21.931	214.16	56.997	171.69	53.464
	2	262.64	85.296	150.65	263.09	61.286	254.28	59.808
	3	460.62	226.56	300.36	539.35	97.939	512.11	97.190
	4	677.35	384.05	505.66	583.42	193.52	580.83	177.09
	5	898.48	581.31	685.43	886.62	359.43	860.50	320.60
[0/90]	1	51.865	8.846	11.239	128.84	48.745	112.12	46.682
	2	141.13	45.614	82.267	174.40	59.679	167.82	58.532
	3	267.66	129.77	179.62	371.09	83.032	348.96	82.089
	4	422.68	240.35	324.54	397.31	130.95	393.14	130.60
	5	597.93	378.64	469.09	633.42	220.11	586.10	213.05
[0/90/0]	1	102.10	17.923	21.640	216.71	56.984	172.22	53.410
	2	262.42	84.886	150.17	254.95	61.292	248.28	59.810
	3	465.29	227.31	300.04	547.94	97.685	518.58	97.038
	4	690.84	383.60	506.01	550.78	193.14	539.92	176.80
	5	920.99	576.64	653.50	867.54	362.43	833.45	322.23
[0/90/0/90]	1	72.274	12.514	15.476	167.75	53.351	138.49	50.262
	2	192.11	62.109	110.87	208.30	60.627	201.28	59.339
	3	353.63	172.04	232.27	450.34	89.398	423.16	89.277
	4	542.19	303.71	406.54	454.42	155.25	445.22	150.87
	5	744.91	464.35	547.68	729.13	280.43	687.52	260.79

Table 6. Frequencies (first five modes) for a paraboloidal curved laminated composite beam with diverse lamination schemes and boundary conditions.

Lamination Schemes (°)	f (Hz)	Boundary Conditions						
		F-F	F-C	SS-SD	C-C	E1-E1	E2-E2	E3-E3
[0]	1	373.52	64.623	164.28	371.90	85.164	322.36	82.579
	2	800.98	312.45	507.90	657.91	87.915	607.76	87.789
	3	1253.6	707.78	881.86	1036.3	210.21	997.29	175.46
	4	1714.7	1110.7	1167.5	1424.0	552.63	1401.6	464.38
	5	2242.4	1181.7	1455.7	1859.1	964.69	1843.9	867.60
[0/90]	1	197.02	32.159	87.238	245.62	81.521	197.89	77.791
	2	491.20	185.02	320.31	469.30	87.631	420.62	87.597
	3	857.49	468.35	641.00	790.40	149.76	710.61	147.49
	4	1275.6	817.64	769.92	1149.3	349.65	1105.4	321.28
	5	1593.7	834.84	1048.4	1518.4	667.48	1415.6	612.78
[0/90/0]	1	373.15	63.977	163.75	358.74	85.290	300.87	82.653
	2	817.30	316.41	512.27	664.06	87.895	602.30	87.767
	3	1292.5	725.21	830.90	1058.7	209.82	1013.9	175.42
	4	1775.5	962.32	1061.6	1460.7	562.24	1437.0	468.36
	5	1921.2	1169.0	1464.0	1848.6	994.58	1841.3	888.14
[0/90/0/90]	1	270.67	45.008	119.10	290.34	83.809	237.39	80.442
	2	635.86	242.33	406.68	554.66	87.796	496.35	87.709
	3	1055.0	583.18	731.14	905.41	172.60	841.77	161.38
	4	1498.5	844.42	897.74	1277.4	442.01	1249.1	385.83
	5	1673.8	974.15	1237.1	1626.3	813.80	1588.1	733.36

Table 7. Frequencies (first five modes) for a hyperbolic curved laminated composite beam with diverse lamination schemes and boundary conditions.

Lamination Schemes (°)	f (Hz)	Boundary Conditions						
		F-F	F-C	SS-SD	C-C	E1-E1	E2-E2	E3-E3
[0]	1	304.37	63.190	84.575	516.70	83.783	454.97	82.037
	2	706.30	215.16	437.29	896.56	84.652	867.29	82.866
	3	1133.2	599.33	851.70	1121.3	201.41	1098.4	169.28
	4	1564.2	1018.0	1265.3	1308.2	457.61	1284.3	390.81
	5	1987.4	1414.5	1411.8	1718.8	862.73	1701.3	772.01
[0/90]	1	166.56	31.709	46.314	375.75	81.434	331.10	78.948
	2	446.82	132.13	279.03	689.45	82.951	647.32	82.043
	3	776.96	399.38	585.56	834.51	143.64	739.01	141.75
	4	1162.2	743.98	878.91	1057.0	303.53	999.08	283.67
	5	1537.4	1058.2	988.53	1429.0	608.67	1378.6	561.35
[0/90/0]	1	303.83	62.500	84.171	531.51	83.853	462.71	82.065
	2	719.58	217.47	442.46	881.36	84.665	877.44	82.869
	3	1165.7	610.38	876.96	991.48	200.91	931.96	169.20
	4	1620.2	1050.2	1103.1	1356.6	464.23	1329.0	393.67
	5	2061.9	1277.5	1316.8	1782.3	887.96	1763.4	789.18
[0/90/0/90]	1	225.23	44.300	62.334	446.17	82.850	388.20	80.604
	2	570.08	169.93	352.15	766.94	83.946	757.90	82.550
	3	955.03	493.94	721.36	864.92	165.59	781.68	155.42
	4	1371.1	882.44	1018.6	1184.5	373.57	1146.2	332.75
	5	1760.7	1113.6	1118.4	1572.6	734.99	1541.4	663.31

Several mode shapes of elliptical (Figure A1), paraboloidal (Figure A2), and hyperbolic (Figure A3) CLCBs with different lamination schemes ($[0^\circ/90^\circ/0^\circ]$ and $[30^\circ/-30^\circ/30^\circ/-30^\circ]$) and boundary conditions (C-F and C-C) are presented (see the Appendix A). The material and geometric properties in Figures A1 and A2 are in accordance with those in Tables 5–7, respectively. To demonstrate the material properties, the mode shapes of isotropic beams (elliptical, paraboloidal, and hyperbolic) are also given in Figures A1–A3. The material properties of the isotropic beams are $\rho = 1500 \text{ kg/m}^3$, $E = 100 \text{ GPa}$, and $\mu = 0.25$. The following aspects should be noted. First, for all the cases, the mode shapes for laminated composite beams and isotropic beams are different. With regard to the F-C boundary condition, obvious differences can be observed for the first-order mode, while for the C-C boundary condition, the mode shapes are similar for the first- and second-order modes, although distinct differences can be observed for the third-order mode. Secondly, with various radii of curvature changes and boundary conditions, the corresponding mode shapes are also quite different. Thirdly, by choosing different lamination schemes, the material properties change, leading to variations in mode shapes of the CLCBs. By properly selecting the lamination schemes, high strength ratio and corrosion resistance can be obtained, which may make the laminated composite materials perform better than others.

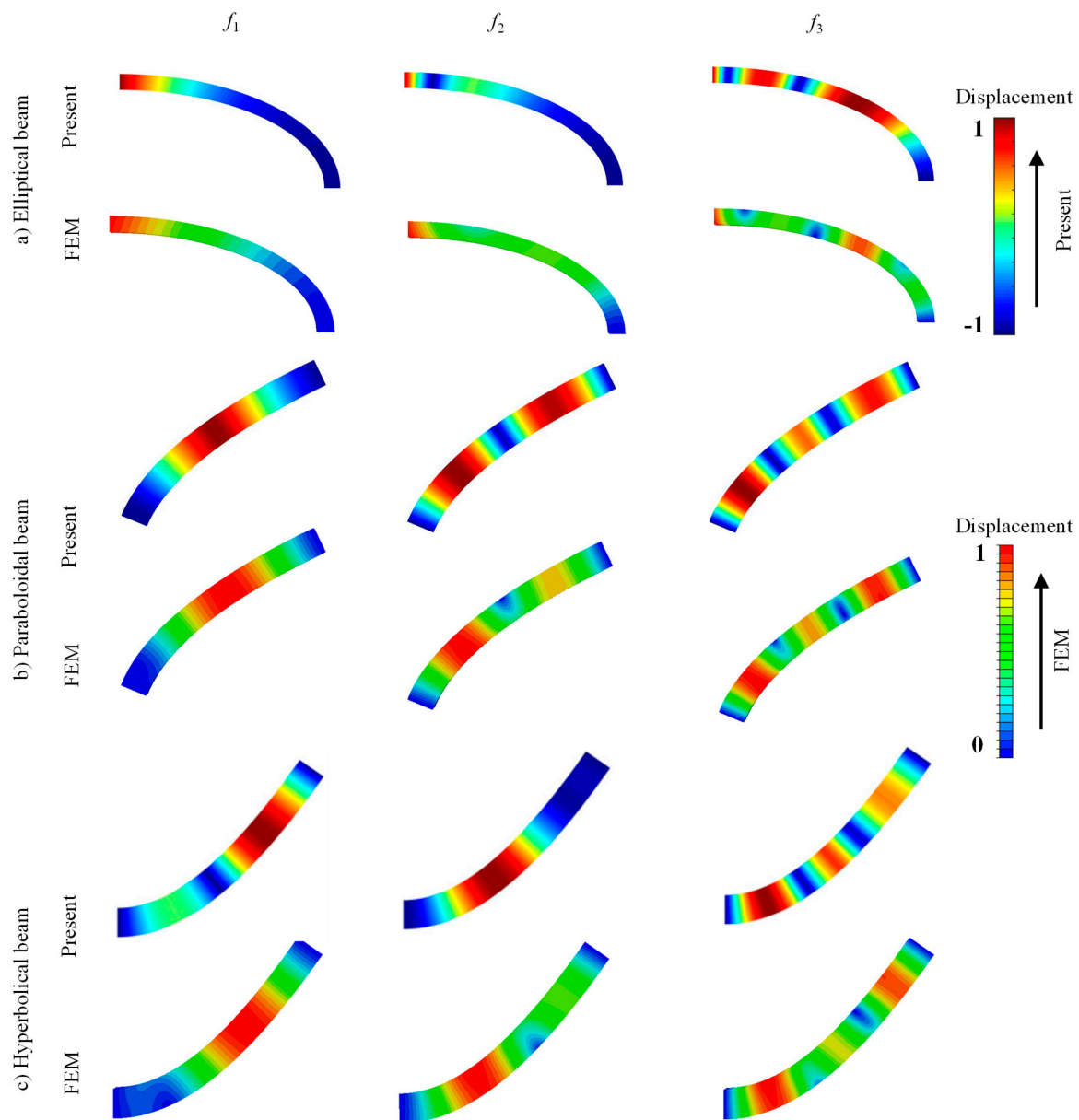


Figure 7. Several mode shapes in x - z plane for CLCBs: (a) Elliptical beam, (b) paraboloidal beam, and (c) hyperbolic beam.

4. Conclusions

This paper proposes a unified formulation for dynamic analysis of different types of CLCBs subjected to general boundary conditions. In the framework of HSDT, an improved variational approach along with a multi-segment partitioning technique is exploited to construct the theoretical model. The displacement components of each curved beam segment are presented in terms of Jacobi orthogonal polynomials. Through a series of numerical cases, the fast convergence performance and stable, highly efficient, and precise features of the current methodology have been demonstrated. It has been proved that the present methodology can be applicable for vibration cases with respect to both classic and elastic boundary conditions. Furthermore, it should be noted that the current approach leads to flexible choices of admissible displacement functions, which is one prominent advantage compared to other methods. This paper presents the free vibration results, while the dynamic analysis of CLCBs under external excitation by the present approach has not been studied. Besides, linear geometric analysis of CLCBs by a unified formulation has been conducted. The present approach

should also be appropriate for non-linear geometric analysis of CLCBs by considering the non-linear geometric effect (e.g., introducing the damping force). These will be considered in our future study.

Author Contributions: Conceptualization, X.Z.; validation, H.L. and Y.Y.; formal analysis, B.Q.; writing—original draft preparation, B.Q.; writing—review and editing, X.Z. and Q.W.; funding acquisition, B.Q., X.Z. and Q.W. All authors have read and agree to the published version of the manuscript.

Funding: This research was funded by the National Natural Science Foundation of China (grant number 11902368, 51705537), the Natural Science Foundation of Hunan Province of China (grant number 2018JJ3661), Innovation Driven Program of Central South University (grant number 2019CX006). The authors also gratefully acknowledge the supports from State Key Laboratory of High Performance Complex Manufacturing, Central South University, China (grant number ZZYJKT2018-18) and from the Graduate Student Independent Innovation Project of Central South University (grant number 2019zzts540).

Conflicts of Interest: The authors declare no conflict of interest.

Appendix A

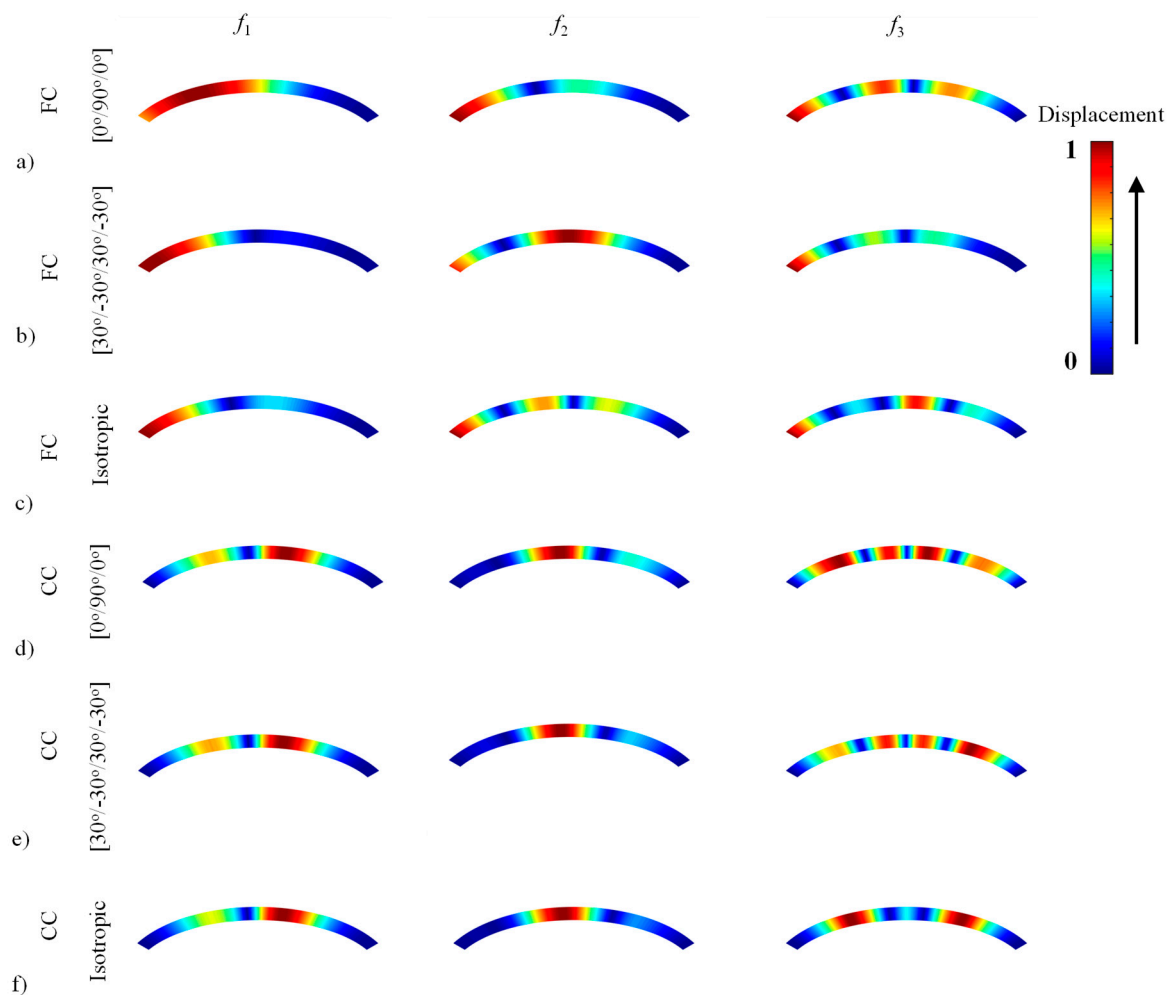


Figure A1. Several mode shapes for an elliptical composite laminated beam and an elliptical isotropic beam.

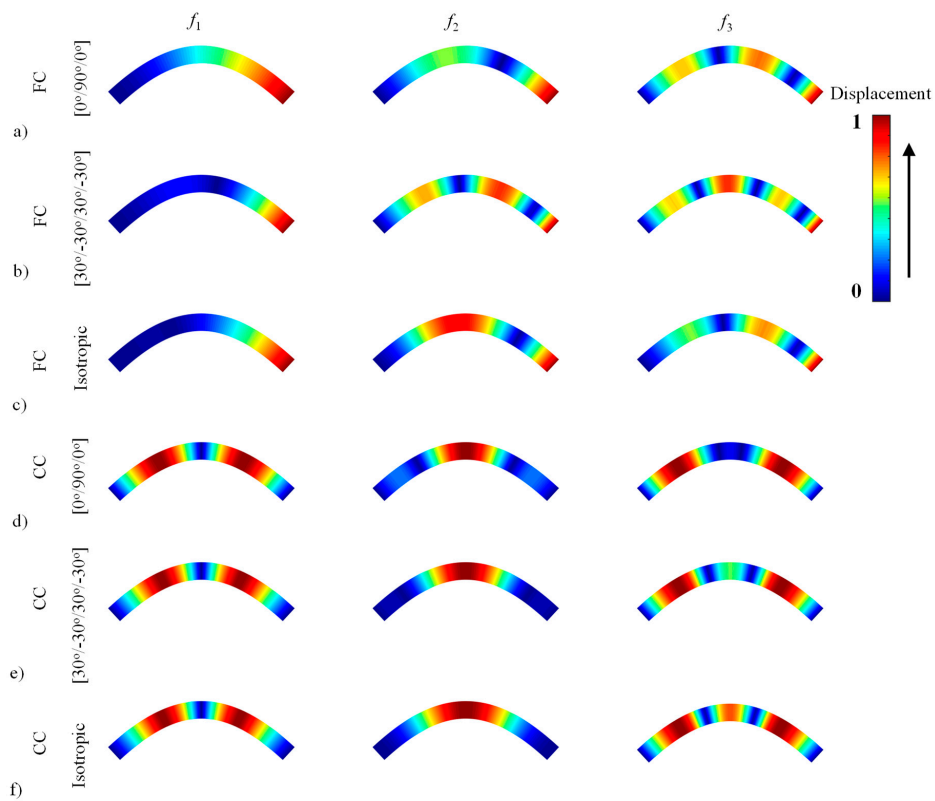


Figure A2. Several mode shapes for a paraboloidal composite laminated beam and a paraboloidal isotropic beam.

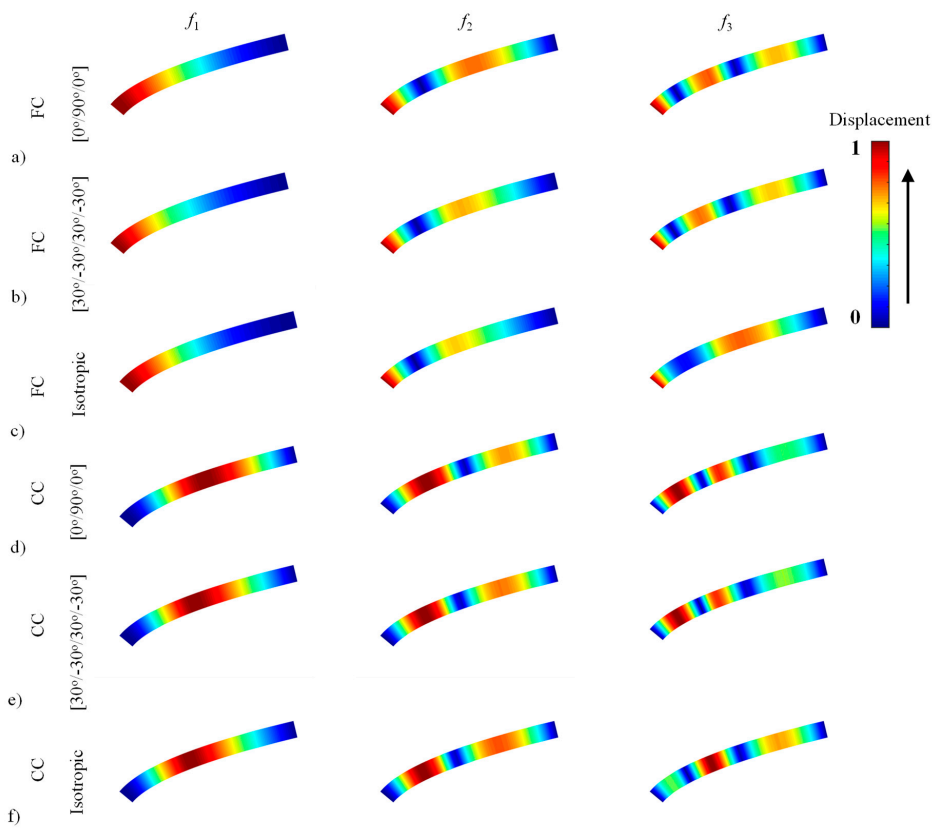


Figure A3. Several mode shapes for a hyperbolical composite laminated beam and a hyperbolical isotropic beam.

References

1. Huu Quoc, T.; Minh Tu, T.; Van Tham, V. Free vibration analysis of smart laminated functionally graded CNT reinforced composite plates via new four-variable refined plate theory. *Materials* **2019**, *12*, 3675. [[CrossRef](#)]
2. Tornabene, F.; Fantuzzi, N.; Baccocchi, M. Linear static behavior of damaged laminated composite plates and shells. *Materials* **2017**, *10*, 811. [[CrossRef](#)] [[PubMed](#)]
3. Qatu, M.S. Theories and analyses of thin and moderately thick laminated composite curved beams. *Int. J. Solids Struct.* **1993**, *30*, 2743–2756. [[CrossRef](#)]
4. Qatu, M.S. In-plane vibration of slightly curved laminated composite beams. *J. Sound Vib.* **1992**, *159*, 327–338. [[CrossRef](#)]
5. Qatu, M.S.; Elsharkawy, A.A. Vibration of laminated composite arches with deep curvature and arbitrary boundaries. *Comput. Struct.* **1993**, *47*, 305–311. [[CrossRef](#)]
6. Tseng, Y.P.; Huang, C.S.; Kao, M.S. In-plane vibration of laminated curved beams with variable curvature by dynamic stiffness analysis. *Compos. Struct.* **2000**, *50*, 103–114. [[CrossRef](#)]
7. Carpentieri, G.; Tornabene, F.; Ascione, L.; Fraternali, F. An accurate one-dimensional theory for the dynamics of laminated composite curved beams. *J. Sound Vib.* **2015**, *336*, 96–105. [[CrossRef](#)]
8. Khdeir, A.A.; Reddy, J.N. Free and forced vibration of cross-ply laminated composite shallow arches. *Int. J. Solids Struct.* **1997**, *34*, 1217–1234. [[CrossRef](#)]
9. Surana, K.S.; Nguyen, S.H. Two-dimensional curved beam element with higher-order hierarchical transverse approximation for laminated composites. *Comput. Struct.* **1990**, *36*, 499–511. [[CrossRef](#)]
10. Hajianmaleki, M.; Qatu, M.S. Static and vibration analyses of thick, generally laminated deep curved beams with different boundary conditions. *Compos. Part B-Eng.* **2012**, *43*, 1767–1775. [[CrossRef](#)]
11. Jafari-Talookolaei, R.-A.; Abedi, M.; Hajianmaleki, M. Vibration characteristics of generally laminated composite curved beams with single through-the-width delamination. *Compos. Struct.* **2016**, *138*, 172–183. [[CrossRef](#)]
12. Chen, W.Q.; Lv, C.F.; Bian, Z.G. Elasticity solution for free vibration of laminated beams. *Compos. Struct.* **2003**, *62*, 75–82. [[CrossRef](#)]
13. Ascione, L.; Fraternali, F. A penalty model for the analysis of curved composite beams. *Comput. Struct.* **1992**, *45*, 985–999. [[CrossRef](#)]
14. Ye, T.; Jin, G.; Ye, X.; Wang, X. A series solution for the vibrations of composite laminated deep curved beams with general boundaries. *Compos. Struct.* **2015**, *127*, 450–465. [[CrossRef](#)]
15. Luu, A.-T.; Kim, N.-I.; Lee, J. NURBS-based isogeometric vibration analysis of generally laminated deep curved beams with variable curvature. *Compos. Struct.* **2015**, *119*, 150–165. [[CrossRef](#)]
16. Shao, D.; Hu, S.; Wang, Q.; Pang, F. A unified analysis for the transient response of composite laminated curved beam with arbitrary lamination schemes and general boundary restraints. *Compos. Struct.* **2016**, *154*, 507–526. [[CrossRef](#)]
17. Qu, Y.; Long, X.; Li, H.; Meng, G. A variational formulation for dynamic analysis of composite laminated beams based on a general higher-order shear deformation theory. *Compos. Struct.* **2013**, *102*, 175–192. [[CrossRef](#)]
18. Garcia, C.; Trendafilova, I.; Zucchelli, A. The effect of polycaprolactone nanofibers on the dynamic and impact behavior of glass fibre reinforced polymer composites. *J. Compos. Sci.* **2018**, *2*, 43. [[CrossRef](#)]
19. Garcia, C.; Wilson, J.; Trendafilova, I.; Yang, L. Vibratory behaviour of glass fibre reinforced polymer (GFRP) interleaved with nylon nanofibers. *Compos. Struct.* **2017**, *176*, 923–932. [[CrossRef](#)]
20. Yagci, B.; Filiz, S.; Romero, L.L.; Ozdoganlar, O.B. A spectral-Tchebychev technique for solving linear and nonlinear beam equations. *J. Sound Vib.* **2009**, *321*, 375–404. [[CrossRef](#)]
21. Bediz, B. Three-dimensional vibration behavior of bi-directional functionally graded curved parallelepipeds using spectral Tchebychev approach. *Compos. Struct.* **2018**, *191*, 100–112. [[CrossRef](#)]
22. Bediz, B.; Aksoy, S. A spectral-Tchebychev solution for three-dimensional dynamics of curved beams under mixed boundary conditions. *J. Sound Vib.* **2018**, *413*, 26–40. [[CrossRef](#)]
23. Tornabene, F.; Fantuzzi, N.; Baccocchi, M.; Viola, E. Accurate inter-laminar recovery for plates and doubly-curved shells with variable radii of curvature using layer-wise theories. *Compos. Struct.* **2015**, *124*, 368–393. [[CrossRef](#)]
24. Qu, Y.; Chen, Y.; Long, X.; Hua, H.; Meng, G. Free and forced vibration analysis of uniform and stepped circular cylindrical shells using a domain decomposition method. *Appl. Acoust.* **2013**, *74*, 425–439. [[CrossRef](#)]

25. Qu, Y.; Hua, H.; Meng, G. A domain decomposition approach for vibration analysis of isotropic and composite cylindrical shells with arbitrary boundaries. *Compos. Struct.* **2013**, *95*, 307–321. [[CrossRef](#)]
26. Qu, Y.; Long, X.; Yuan, G.; Meng, G. A unified formulation for vibration analysis of functionally graded shells of revolution with arbitrary boundary conditions. *Compos. Part B-Eng.* **2013**, *50*, 381–402. [[CrossRef](#)]
27. Qu, Y.; Chen, Y.; Chen, Y.; Long, X.; Hua, H.; Meng, G. A Domain Decomposition Method for Vibration Analysis of Conical Shells With Uniform and Stepped Thickness. *J. Vib. Acoust.* **2013**, *135*, 011014. [[CrossRef](#)]
28. Qin, B.; Zhong, R.; Wang, T.; Wang, Q.; Xu, Y.; Hu, Z. A unified Fourier series solution for vibration analysis of FG-CNTRC cylindrical, conical shells and annular plates with arbitrary boundary conditions. *Compos. Struct.* **2020**, *232*, 111549. [[CrossRef](#)]
29. Zhang, H.; Zhu, R.; Shi, D.; Wang, Q.; Yu, H. Study on vibro-acoustic property of composite laminated rotary plate-cavity system based on a simplified plate theory and experimental method. *Int. J. Mech. Sci.* **2020**, *167*, 105264. [[CrossRef](#)]
30. Ye, T.; Jin, G.; Su, Z. A spectral-sampling surface method for the vibration of 2-D laminated curved beams with variable curvatures and general restraints. *Int. J. Mech. Sci.* **2016**, *110*, 170–189. [[CrossRef](#)]
31. Liu, T.; Wang, A.; Wang, Q.; Qin, B. (2020) Wave Based Method for Free Vibration Characteristics of Functionally Graded Cylindrical Shells with Arbitrary Boundary Conditions. *Thin-Walled Struct.* **2020**, *148*, 106580. [[CrossRef](#)]
32. Choe, K.; Tang, J.; Shui, C.; Wang, A.; Wang, Q. Free vibration analysis of coupled functionally graded (FG) doubly-curved revolution shell structures with general boundary conditions. *Compos. Struct.* **2018**, *194*, 413–432. [[CrossRef](#)]
33. Choe, K.; Wang, Q.; Tang, J.; Shui, C. Vibration analysis for coupled composite laminated axis-symmetric doubly-curved revolution shell structures by unified Jacobi-Ritz method. *Compos. Struct.* **2018**, *194*, 136–157. [[CrossRef](#)]
34. Wang, Q.; Choe, K.; Shi, D.; Sin, K. Vibration analysis of the coupled doubly-curved revolution shell structures by using Jacobi-Ritz method. *Int. J. Mech. Sci.* **2018**, *135*, 517–531. [[CrossRef](#)]
35. Shao, D.; Hu, S.; Wang, Q.; Pang, F. Free vibration of refined higher-order shear deformation composite laminated beams with general boundary conditions. *Compos. Part B-Eng.* **2017**, *108*, 75–90. [[CrossRef](#)]



© 2020 by the authors. Licensee MDPI, Basel, Switzerland. This article is an open access article distributed under the terms and conditions of the Creative Commons Attribution (CC BY) license (<http://creativecommons.org/licenses/by/4.0/>).